

Electrostatic Actuating Double-Unit Electrocaloric Cooling Device with High Efficiency

Yiwen Bo, Quan Zhang, Heng Cui, Mengyan Wang, Chunyang Zhang, Wen He, Xiangqian Fan, Yiwen Lv, Xiang Fu, Jiajie Liang, Yi Huang, Rujun Ma,* and Yongsheng Chen

Compact solid-state refrigeration systems that offer a high specific cooling power and a high coefficient of performance (COP) are desirable in a wide range of applications where efficient and localized heat transfer is required. Here, a double-unit electrocaloric (EC) polymer-based refrigeration device with high intrinsic thermodynamic efficiency is demonstrated using a flexible EC polymer film with improved performance by doping plasticizer and an electrostatic actuation mechanism. The double-unit refrigeration device achieves a large temperature span of 4.8 K, which is 71% higher than that of the single-unit device. A specific cooling power of 3.6 W g^{-1} and a maximum COP of 8.3 for the cooling device are produced. The surface temperature of a central processing unit (CPU) cooled by an active EC device is 22.4 K lower than that of the CPU cooled in air. The highly efficient and compact EC cooling device demonstrated here not only leapfrogs the performance of existing solid-state cooling technologies, but also brings solid state cooling closer to reality for a variety of practical applications that require compact or mechanically flexible refrigeration.

of chip operating temperature to avoid overheating is an important guarantee to maintain the normal operation of electronic devices. The traditional refrigeration technology based on the vapor compression cycle is difficult to meet the refrigeration requirements of highly integrated microelectronic devices due to the existence of the compressor.^[2] Moreover, the extensive use of chlorofluorocarbons and other refrigerants bring about new problems such as ozone layer destruction and greenhouse effect, and the relatively low coefficient of performance (COP) also limits its application in cooling systems for electronic devices.^[3] Therefore, it is necessary to develop a new type of refrigeration technology that can be miniaturized, high efficiency, and environment-friendly.

Solid-state refrigeration technology as an alternative has the properties of no heat transfer media of liquid refrigerants, rapid cooling, safety, and environmental protection.^[2] The existing solid-state refrigeration technologies include thermoelectric, magnetocaloric, elastocaloric, and electrocaloric (EC) refrigeration technologies. Thermoelectric refrigerators fabricated by bismuth antimony telluride ceramics have a variety of applications.^[4–6] However, their COP is lower than that of vapor compression coolers.^[7] Magnetocaloric and elastocaloric coolers require a strong magnetic field and high load to achieve the entropy change of the refrigeration material, respectively, which limits their miniaturization.^[8,9] The EC cooling technology has been considered to be a more effective alternative and can also be used to realize compact and low-profile devices. The EC effect is the change of internal polarization state caused by the change of external electric field under adiabatic condition, which leads to the change of entropy and temperature.^[10] The current generated in the cooling process is quite small and energy consumption is very low due to the insulation of materials. Therefore, compared with other solid-state refrigeration technologies, EC refrigeration is not only environmentally friendly and efficient, but also has an important application prospect in the temperature regulation of microelectronic devices.


Current EC materials of relaxor ferroelectric ceramics have promising performance. However, EC refrigeration devices based on ferroelectric ceramics are limited by the inherent

1. Introduction

Nowadays, with the development of electronic chips to high frequency and miniaturization, the failure of electronic devices is becoming more and more prominent due to the improvement of its integration. Failure problems caused by device overheating accounted for about 55% among all the failure phenomena of electronic devices.^[1] Therefore, the effective control

Y. Bo, Dr. Q. Zhang, H. Cui, M. Wang, C. Zhang, Dr. W. He, X. Fan, Y. Lv, X. Fu, Prof. J. Liang, Prof. Y. Huang, Prof. R. Ma
School of Materials Science and Engineering
National Institute for Advanced Materials
Tianjin Key Lab for Rare Earth Materials and Applications
Nankai University
Tongyan Road 38, Tianjin 300350, P. R. China
E-mail: malab@nankai.edu.cn

Prof. Y. Chen
State Key Laboratory and Institute of Elemento-Organic Chemistry
Centre of Nanoscale Science and Technology and Key Laboratory of
Functional Polymer Materials
College of Chemistry
Nankai University
Tianjin 300071, P. R. China

 The ORCID identification number(s) for the author(s) of this article can be found under <https://doi.org/10.1002/aenm.202003771>.

DOI: 10.1002/aenm.202003771

brittleness of the materials.^[11–13] It is necessary to use an external motor to drive solid parts or pump fluid media to achieve directional heat transfer, which reduces the COP of the device and increases the complexity of the cooling system.^[14–17] Compared with the ferroelectric polymer poly(vinylidene fluoride-trifluoroethylene) [P(VDF-TrFE)], Curie temperature of the relaxor ferroelectric terpolymer poly(vinylidene fluoride-trifluoroethylene-ter-chloroethylene) [P(VDF-TrFE-CFE)] is near room temperature. The adiabatic temperature change of 12 K and isothermal entropy change of $55 \text{ J (kg} \cdot \text{K)}^{-1}$ have been calculated.^[18,19] A compact and single-unit solid-state refrigeration device was developed using P(VDF-TrFE-CFE) with the specific cooling power of 2.8 W g^{-1} and temperature span of 2.8 K by electrostatic actuation,^[20] and a cascade EC cooling device with larger temperature lift was also investigated.^[21] However, P(VDF-TrFE-CFE) as the core EC material of the device requires a large external electric field to reach high adiabatic temperature change. This is related to the need to overcome the interaction between the molecular chains when the dipole is oriented under the action of an electric field.^[22] Therefore, it is necessary to further improve the EC performance of the materials, so that it can generate a larger temperature change under a lower electric field, thereby improving the cooling ability of the device. Great efforts have been made to disperse inorganic materials, such as $(1-x)\text{Pb}(\text{Mg}_{1/3}\text{Nb}_{2/3})\text{O}_3-x\text{PbTiO}_3$ nanoparticles,^[23] $\text{Ba}_x\text{Sr}_{1-x}\text{TiO}_3$ with different aspect ratio,^[24] graphene,^[25] $\text{BaZr}_{0.21}\text{Ti}_{0.79}\text{O}_3$ nanofibers,^[26] $\text{BaZr}_{0.21}\text{Ti}_{0.79}\text{O}_3$ nanofibers embedded with BiFeO_3 nanoparticles,^[27] in the P(VDF-TrFE-CFE) matrix to form nanocomposites which can greatly improve the EC performance and thermal conductivity. However, good dispersion of inorganic materials in the EC polymer is the key to improving EC performance of composite materials. Meanwhile, the addition of inorganic materials reduces the flexibility of the EC polymer. Moreover, EC performance can also be enhanced by adjusting the component ratio of the mixture of P(VDF-TrFE) and P(VDF-TrFE-CFE).^[28,29] Nevertheless, the research on modification of P(VDF-TrFE-CFE), especially in the field of flexible refrigeration devices, is still insufficient. In addition, the optimization of the EC refrigeration-device architecture is also necessary to further improve the cooling performance of the device.

Here, we report a double-unit solid-state refrigeration device using electrostatic force to achieve the rapid motion of two modified EC polymer stacks to pump heat. Thanks to the light weight of the EC polymer stack, electrostatic forces can rapidly transport the S-shaped EC polymer stack while promoting intimate thermal contact between the EC material and the heat source/heat sink. Dioctyl phthalate (DOP) with benzene ring and long chain structure acts as an interchain lubricant in P(VDF-TrFE-CFE) to reduce the steric hindrance during the movement of molecular chains and improves the crystallinity. Compared with pure P(VDF-TrFE-CFE), the required electric field for DOP-modified polymer with temperature change of 7 K decreases by 28.5 MV m^{-1} . Moreover, the compact double-unit electrostatic-actuated EC cooling device ($6 \text{ cm} \times 3 \text{ cm} \times 0.8 \text{ cm}$) using modified P(VDF-TrFE-CFE) polymer stacks achieves a larger temperature span of 4.8 K, which is 71% higher than that of the single-unit EC cooling device. Even after 4500 times of charge and discharge, the EC performance of the cooling

device is basically unchanged. Higher temperature change can be reached by the multi-unit EC cooling device according to the demand of device refrigeration. Combined with feedback circuit, the device can automatically control the temperature of central processing unit (CPU) anytime. Simple material modification methods, miniaturized structural design, and low energy consumption operation requirements provide the possibility for EC refrigeration technology to solve overheating problem in the field of integrated electronic devices.

2. Results and Discussion

We chose DOP-modified P(VDF-TrFE-CFE) as the active EC material to prepare EC polymer stacks because of large entropy change, large temperature change near room temperature, good flexibility, and easy processability.^[18] Pre-dissolved P(VDF-TrFE-CFE) solution containing DOP was blade-coated onto a clean glass substrate and the resulting film was heated in a vacuum oven at $90 \text{ }^\circ\text{C}$ for 3 h to fully evaporate solvent. Single-walled carbon nanotubes (CNT)-based isopropyl-water dispersion was spray-coated on the EC polymer to form a conductive network. Then, another EC polymer layer was directly fabricated on the CNT network by blade-coating polymer solution. It should be noted that a part of CNT network was uncovered with the second EC polymer in order to connect with power source in control circuit. After peeling off the film from glass substrate, CNT dispersion was also spray-coated on the rest of two surface of the polymer to achieve a complete two-layer EC polymer stack. The overlap of three CNT-based electrodes across the polymer films was defined as active area ($2 \text{ cm} \times 4 \text{ cm}$ in size) for the EC effect. Finally, as-prepared EC polymer stack was annealed in a vacuum oven at $120 \text{ }^\circ\text{C}$ for 10 h, to which increase the degree of crystallinity and improve the polarizability of the polymer (Figure 1a and Figure S1, Supporting Information).^[30] From the cross-section SEM image, a clear boundary between two EC polymer layers is observed and the thickness of each layer is the same $35 \text{ }\mu\text{m}$ (Figure 1b).

In previous work, pure P(VDF-TrFE-CFE) has been demonstrated to be an excellent candidate EC polymer in a single-unit refrigeration device.^[20] However, this polymer must be in a high electric field to have considerable EC performance.^[31] The reason is that the polarization in EC polymer materials is caused by the dipole moment rotation of the molecular chains. Compared with EC ceramic materials, the polarization amplitude in EC polymer materials is smaller. Thus, a higher electric field is required to trigger.^[32] Therefore, we mixed a small amount of plasticizer DOP into P(VDF-TrFE-CFE). On the one hand, for a small amount of added plasticizer, the plasticizer molecules restrict the rotation of the short segments in polymer molecular chain, which is conducive to improve the degree of crystallinity of the EC polymer. This phenomenon is defined as anti-plasticization (Figure S2, Supporting Information).^[33] On the other hand, dipole-dipole interaction often occurs between ester group-containing plasticizers (DOP) and polymers.^[34] This interaction tends to align the molecules to increase attraction, which may help to increase the spontaneous polarization of EC polymer. Larger spontaneous polarization is conducive to the improvement of the EC performance of the EC polymer.^[28]

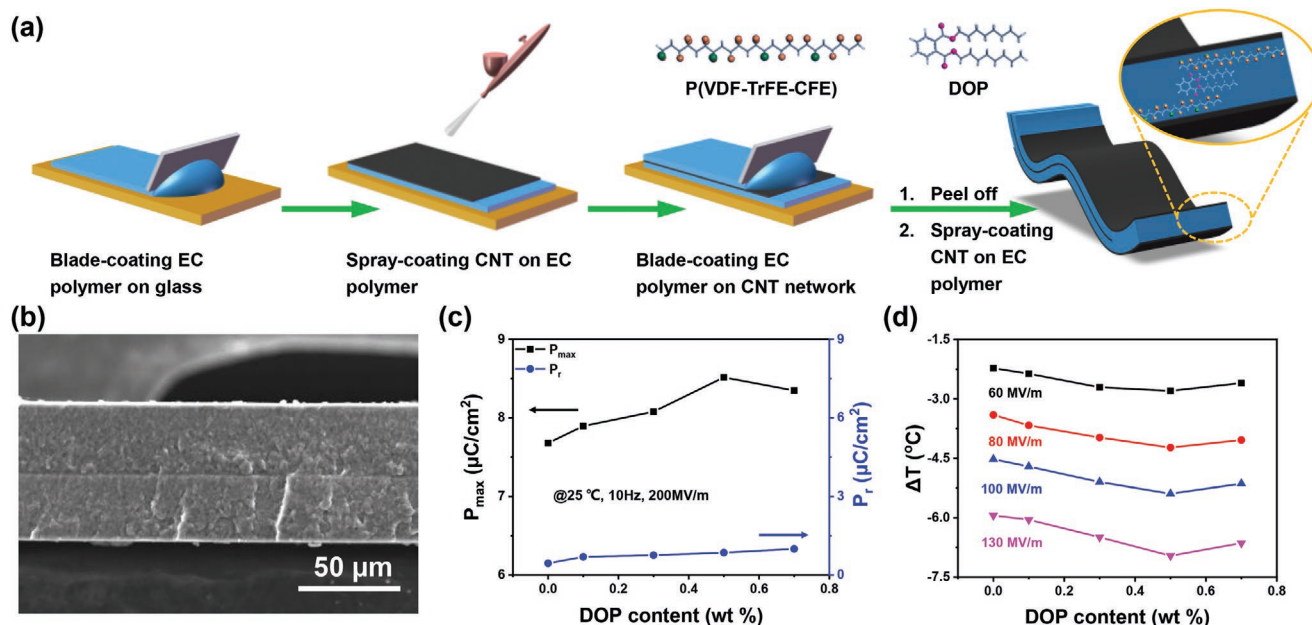


Figure 1. A two-layer EC polymer stack with high performance. a) Schematic illustration of preparation process of two-layer EC polymer stack. b) Cross-section morphology of a 70- μm -thick two-layer EC polymer stack. The scale bar is 50 μm . c) Maximum polarization and remnant polarization of modified P(VDF-TrFE-CFE) as a function of DOP content. The results are measured under electric field of 200 MV m^{-1} at 10 Hz at room temperature (25 $^{\circ}\text{C}$). d) Temperature change (ΔT) of modified P(VDF-TrFE-CFE) with various mass fraction of DOP under a different electric field at room temperature.

The synergistic effect between the improvement of crystalline and enhancement of spontaneous polarization could reduce the required electric field for the EC effect in DOP-modified P(VDF-TrFE-CFE).

Figure 1c shows maximum polarization and remnant polarization of EC film as a function of DOP content. As the DOP content (mass fraction) increases from 0 to 0.7%, the maximum polarization first increases and then decreases, and the inflection point is 0.5% (Figures S3 and S4, Supporting Information). This is related to the reduction of crystallinity caused by excessive plasticizer molecules (Figure S1, Supporting Information). The polarizing microscopy images show that the grain size of 0.5 wt%-DOP-modified P(VDF-TrFE-CFE) is slightly reduced compared with pure EC polymer. It improves the EC performance of the EC polymer.^[23,35] With the further increase of the mass fraction of DOP in EC polymer, the degree of crystallinity gradually decreases (Figure S5, Supporting Information). Meanwhile, the remnant polarization (P_r) just slightly increases with the increase of DOP content. The EC effect of DOP-modified P(VDF-TrFE-CFE) under various electric fields was directly measured using an infrared imaging camera (Figure 1d and Figure S6, Supporting Information). When the applied electric field increases from 60 to 130 MV m^{-1} , the temperature change of all DOP-modified P(VDF-TrFE-CFE) increase. Under the same electric field, the temperature change of modified P(VDF-TrFE-CFE) also increases first and then decreases. The inflection point is the same as that of maximum polarization strength of 0.5 wt%. Compared with pure EC polymer, the temperature change of 0.5 wt%-DOP-modified P(VDF-TrFE-CFE) improves by 1 K under the electric field of 130 MV m^{-1} . The EC performance of the 0.5 wt%-DOP-modified P(VDF-TrFE-CFE) is also determined by the environment temperature.

Figure S7, Supporting Information, shows the polarization-electric field loops of the 0.5 wt%-DOP-modified P(VDF-TrFE-CFE) at different temperatures. When the temperature is close the Curie temperature of the EC polymer, there is a slight hysteresis. As the environment temperature increases, the hysteresis phenomenon gradually becomes obvious. It shows that 0.5 wt%-DOP-modified P(VDF-TrFE-CFE) has better EC performance at room temperature. These experimental results indicate that DOP actually reduces the required electric field for the EC effect. According to the EC performance, the two-layer EC polymer stack made of 0.5 wt%-DOP-modified P(VDF-TrFE-CFE) is used to construct the double-unit refrigeration device.

Figure 2a is the schematic illustration of a double-unit refrigeration device based on two-layer EC polymer stacks. In each unit, two 50- μm -thick polyethylene terephthalate (PET) films coated with graphene-paint electrode are separated by two 3-mm-thick polydimethylsiloxane (PDMS) spacers. In the case of upper unit, a two-layer EC polymer stack is mounted at one end of the unit between the left spacer and the upper PET film, and the other end between the right spacer and the lower PET film. The state of two-layer EC polymer stack in lower unit is opposite to that in upper unit. The reason for this design is to improve heat transfer efficiency from one stack to another stack by increasing the overlapping area. The adjacent PET films between each unit share a graphene-paint electrode. Single-sided polyimide (PI) tape covering the outmost graphene-paint-coated PET film in the double-unit refrigeration device is used to electrically insulate the device from the heat source and the heat sink.

In addition, a control circuit was designed to realize the continuous working mode of the double-unit refrigeration device, which is controlled by two independent power supplies

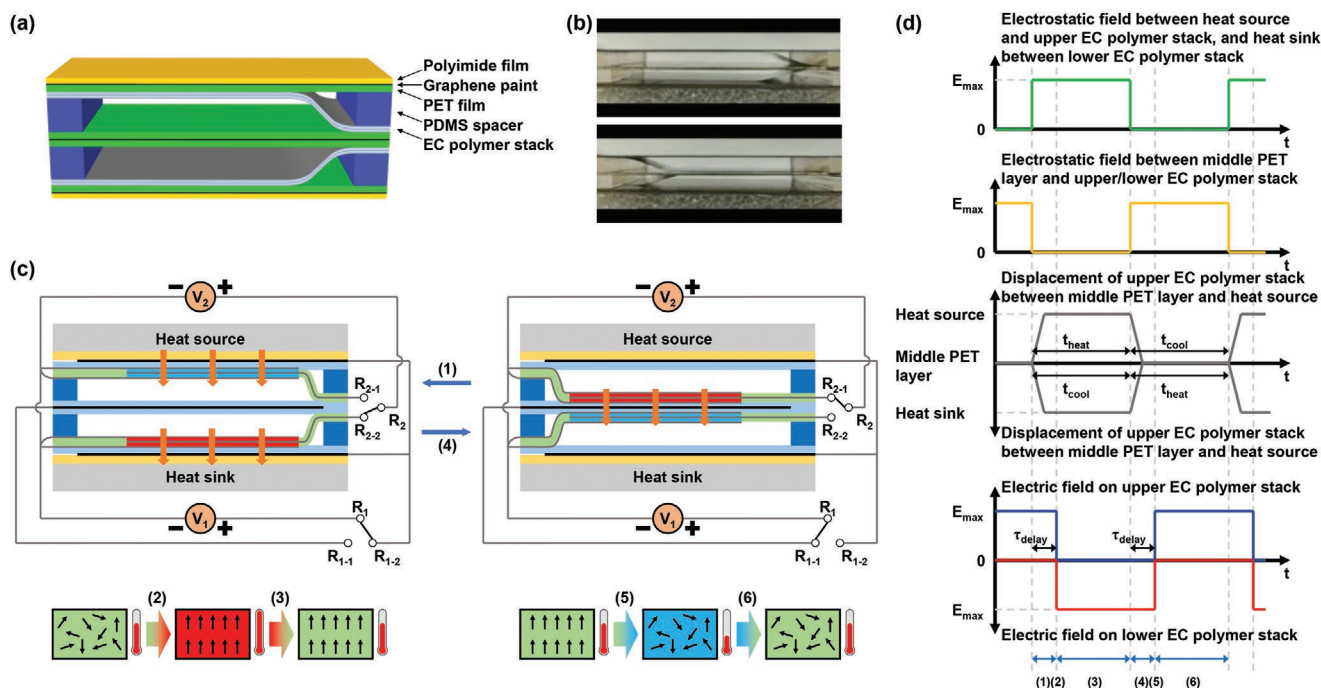


Figure 2. A double-unit refrigeration device and its working mechanism to pump heat from the heat source to the heat sink by electrostatic actuation. a) Schematic illustration of a double-unit refrigeration device. b) Side-view photographs of a double-unit refrigeration device actuated by electrostatic force. Two EC polymer stacks are on the heat source and heat sink, respectively (top), and contact with the middle PET layer together (bottom). c) Schematic illustration of a double-unit device showing how the electrostatic field drives the actuation of the DOP modified EC polymer stack toward the heat sink or heat source and the respective position of the EC polymer film. The bottom schematic illustration shows entropy change of the EC polymer stack in the lower unit during a complete cycle. d) Time-domain illustration of a complete operating cycle of pumping heat from heat source to heat sink.

(Figure 2c). One (V_1) is driving power supply that moves the EC polymer stacks through electrostatic field. The other (V_2) is used to apply the electric field on the EC polymer to produce the EC effect. The two outer CNT electrodes of the EC polymer stacks are used as common cathode, which are connected with the ground terminal of two power supplies by copper wires. The remaining middle CNT electrode of the EC polymer stacks serves as the anode connected with the output terminal of power supply for the EC effect (V_2) by an electric relay (R_2). All the graphene-paint electrodes coated on PET film are connected to the output terminal of driving power supply (V_1) by another electric relay (R_1).

During the operation, both two power supplies provide a continuous output constant voltage. The complete operating cycle of a double-unit refrigeration device pumping heat from the heat source to the heat sink is accomplished in six steps (Figure 2c,d). 1) The EC polymer stacks in the upper and lower unit move to the heat source and the heat sink under the same driving electrostatic field, respectively. By switching the electric relay R_1 to R_{1-2} , an electrostatic field is applied between the top graphene-paint electrode and the outer CNT electrode of the EC polymer stack in upper unit, and between the bottom graphene-paint electrode and the outer CNT electrode of EC polymer stack in lower unit, simultaneously. The electrostatic force moves the upper EC polymer stack to the heat source and holds it there. Meanwhile, the lower EC polymer stack also contacts to the heat sink (top image in Figure 2b). This electrostatic driving force increases thermal contact between the EC polymer stack and the PET, thereby promoting heat transfer

between them (Figure S8, Supporting Information). 2) The EC effect heats the upper EC polymer stack and cools the lower one. When the relay R_2 is switched from R_{2-1} to R_{2-2} , the electric field for the EC effect is applied to the lower polymer stack and removed from the upper one. Due to the aligned dipoles under the effect of the EC effect, the increase of temperature is accompanied by the reduction of entropy in the EC polymer of the lower stacks, while the temperature of the EC polymer in the upper one decreases after removing the electrostatic field. 3) Heat transfers from the heat source to the upper EC polymer stack and from the lower one to the heat sink. Due to the EC heating, a temperature gradient is generated, resulting in heat transfer from the heat source to the upper EC polymer stack. Meanwhile, heat is transferred from the lower EC polymer stack to the heat sink. 4) The upper and lower EC polymer stacks are gathered to the middle PET film under the actuation of electrostatic field. By switching the relay R_1 to R_{1-1} , the driving electrostatic field is removed from the top and bottom graphene-paint electrodes, and applied to the graphene-paint electrode in middle PET film to actuate two EC polymer stacks to contact to the middle PET film together (bottom image in Figure 2b). 5) The EC effect heats the upper EC polymer stack and cools the lower one. As opposed to step 2, when the relay R_2 is switched to R_{2-2} , the temperature of the lower EC polymer stack decreases due to the entropy increase caused by random distribution of dipoles in the polymer after removing the electrostatic field for the EC effect. Meanwhile, the temperature of the upper one increases. 6) Heat transfers from the upper EC polymer stack to the lower one through PET film. Due to

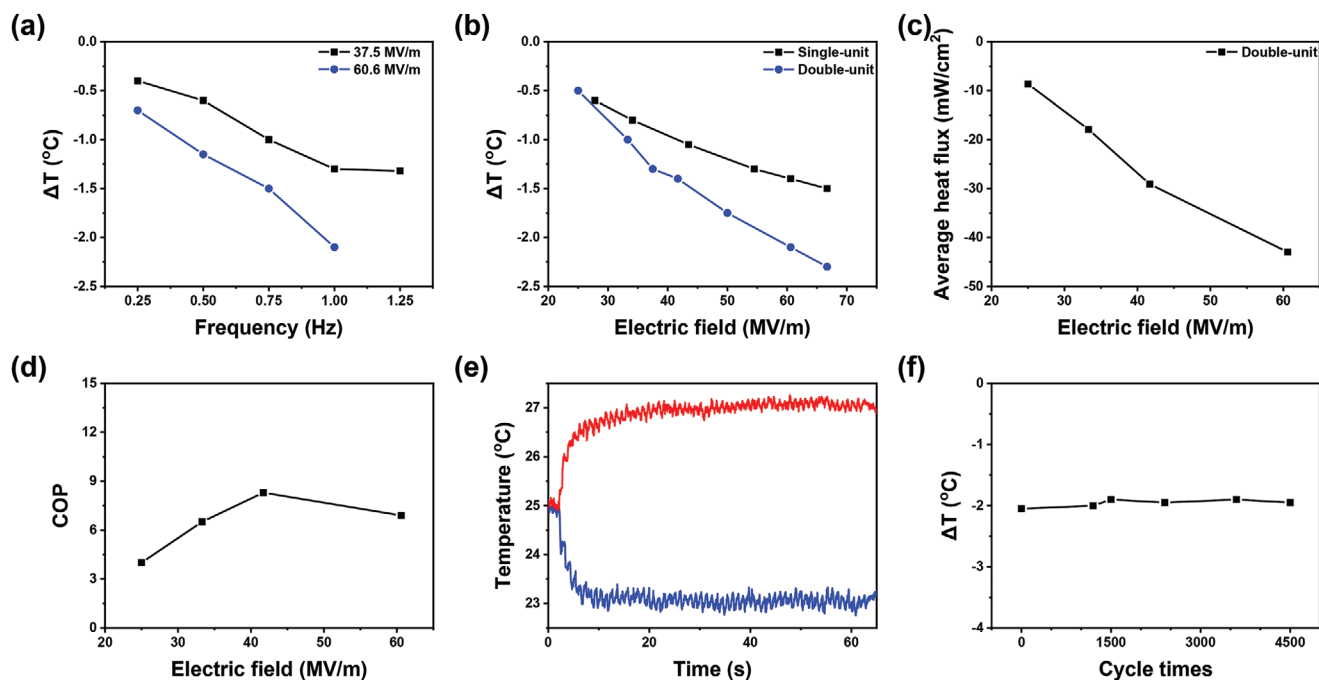


Figure 3. Cooling performance of double-unit refrigeration device. a) Cooling temperature difference of double-unit refrigeration device under different operation frequency and electric field. b) Cooling temperature difference of single-unit and double-unit refrigeration devices under different applied electric field for the EC effect. The corresponding operation frequency is fixed at 1 Hz. c) Heat flux and d) COP of double-unit refrigeration device as a function of different applied electric field at 1.0 Hz of operation frequency. e) Time-resolved temperature span of double-unit refrigeration device placed on an Al block (heat sink). The operation frequency is 1 Hz and the applied electric field of the EC effect is 60.6 MV m⁻¹. f) Temperature difference of cooling during repeated cycles of charging–discharging under the electric field of 60.6 MV m⁻¹ for the EC effect, when the double-unit device works at the frequency of 1 Hz.

the existence of temperature difference, the heat in the upper EC polymer stack absorbed from the heat source is transferred to the lower one in another unit. In this way, the active heat transfer from the heat source to the heat sink is realized (Figure S9, Supporting Information).

In one complete cycle, there are twice EC polymer stack movements and once EC heating and cooling of EC polymer in each unit. In general, the operating steps of the upper and lower unit are the same. The bottom schematic illustration in Figure 2c shows the entropy change process of the EC polymer stack in the lower unit during a complete cycle. In order to better transfer heat from the heat source to the heat sink, the entropy change process of the upper unit is staggered by half of a cycle with the lower unit, namely 1-2-3-4-5-6 for the lower unit and 4-5-6-1-2-3 for the upper unit. It is worth noting that in the whole process, the switching time of relay R₂ is always 0.05 s later than that of relay R₁. This is to form sufficient thermal contact between the EC polymer stacks and the PET film before applying an electric field to the EC polymer film. Due to the unidirectional heat transfer, the heat from the heat source can be continuously transferred to the heat sink by repeating the above steps. Moreover, the double-unit EC cooling device can operate in different frequency (see Videos S1–S4, Supporting Information).

A simulated scene was built to analyze the effect of operating conditions on the cooling performance of refrigeration device. A double-unit refrigeration device (6 cm × 3 cm × 0.8 cm) was placed on an Al block (4 cm × 8 cm × 0.6 cm) used as the heat

sink. The top graphene-paint electrode is regarded as the heat source, which is directly exposed to the air for infrared imaging (Figure S6, Supporting Information). The duration time of steps 3 and 6, equivalent to operation frequency, is an important factor influencing the cooling performance of the double-unit refrigeration device (Figure 3a). As the operation frequency increases, the heat exchange efficiency gradually improves. Even so, when the frequency exceeds 1.0 Hz, there is no further increase of the temperature difference between the heat source and the heat sink. This is related to insufficient heat exchange in steps 3 and 6, because the heat transfer time is shortened. Increasing the electrostatic field for the EC effect is another way to improve the cooling performance of the double-unit refrigeration device. Figure 3b shows that the temperature difference between single-unit and double-unit refrigeration device operated at the same frequency of 1.0 Hz gradually increases with the applied electric field. And the temperature difference of double-unit refrigeration device is always larger than that of the single-unit one under different applied electric fields. Among them, when the electric field for the EC effect is 66.7 MV m⁻¹, the increase of the temperature difference is close to 1 K. Similar to the temperature difference, the heat flux of double-unit device also improves with the increase of applied electric field (Figure 3c). When the device is operated under the electric field of 60.6 MV m⁻¹ at frequency of 1 Hz, the measured heat flux is about 43 mW cm⁻² corresponding to a specific cooling power of 3.6 W g⁻¹. COP is equal to the ratio of heat flux and corresponding electric energy consumption. As shown in Figure 3d,

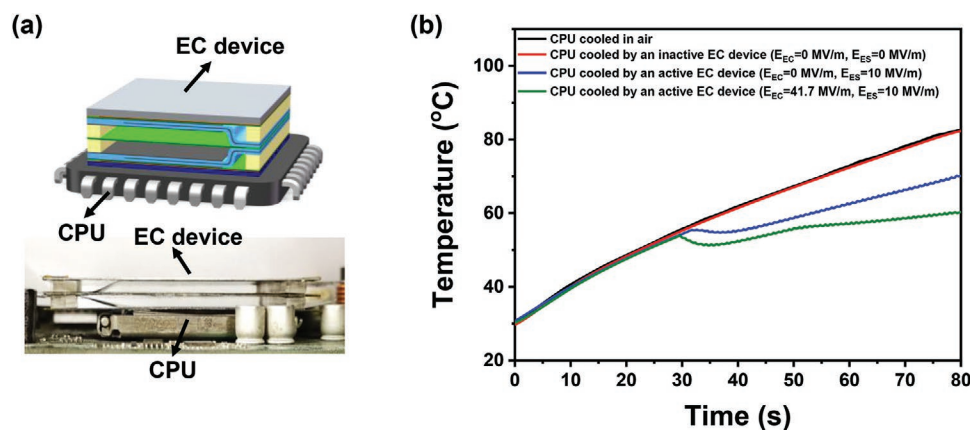


Figure 4. Cooling performance of double-unit refrigeration device for CPU. a) Schematic illustration and photograph of a double-unit EC refrigeration device on a CPU. b) Time-resolved temperature curves of CPU cooled in air (black) and cooled by an inactive EC device ($E_{EC} = 0 \text{ MV m}^{-1}$, $E_{ES} = 0 \text{ MV m}^{-1}$ (red)), active EC device ($E_{EC} = 0 \text{ MV m}^{-1}$, $E_{ES} = 10 \text{ MV m}^{-1}$ (blue)) and active device ($E_{EC} = 41.7 \text{ MV m}^{-1}$, $E_{ES} = 10 \text{ MV m}^{-1}$ (green)). The EC device start-up temperature is $55 \text{ }^{\circ}\text{C}$ considering that a higher temperature will reduce the efficiency of the CPU or even cause failure.

COP increases first and then decreases with the increase of applied electric field and the maximum COP is 8.3 under the electric field of 41.7 MV m^{-1} (Figure S10, Supporting Information). It indicates that there is a great enhancement of electric energy consumption when the applied electric field is larger than 41.7 MV m^{-1} , although large electric field also increases the heat flux of the device. The temperature span of double-unit refrigeration device operating at the frequency of 1 Hz is 4.1 K under the electric field of 60.6 MV m^{-1} , while the temperature span of single-unit device is only 2.8 K (Figure 3e, Figures S11 and S12, Supporting Information). The same temperature difference of heating and cooling indicates that there is almost no leakage current during the device operation. After 4500 cycles, the device does not show any obvious cooling performance degradation (Figure 3f). These results indicate that the cooling performance of EC refrigeration device with this structure can be improved by optimizing operation conditions and increasing the number of units.

Finally, we demonstrated the cooling performance of the double-unit refrigeration device for CPU in practice. The surface temperature of CPU is measured by a surface-mount K-type thermocouple (Figure 4a). Overheating can slowdown the processing power of CPU, shorten service life, and even create a fire hazard. The double-unit refrigeration device can operate at any time combined with an automatic control circuit, when the temperature of cooling object reaches the setting value. The EC device start-up temperature is $55 \text{ }^{\circ}\text{C}$ considering that higher temperature will reduce the efficiency of CPU or even failure. From the moment power on of the CPU, the surface temperature of CPU without the original cooling system rapidly rises from 29.7 to $82.6 \text{ }^{\circ}\text{C}$ in 80 s . As a reference, the temperature of CPU cooled by an inactive EC device is similar to that of CPU cooled in air. In contrast, the final surface temperature of the CPU, cooled by the double-unit refrigeration device operating under applied electric field for EC effect (E_{EC}) of 41.7 MV m^{-1} and electrostatic field (E_{ES}) of 10 MV m^{-1} at 1 Hz is stabilized at $60.2 \text{ }^{\circ}\text{C}$. When EC device is operated by electrostatic force and without EC field ($E_{EC} = 0 \text{ MV m}^{-1}$ and $E_{ES} = 10 \text{ MV m}^{-1}$), the final temperature of the CPU is $70.3 \text{ }^{\circ}\text{C}$. It indicates EC effect

further improves the cooling performance of the EC device, although the device operating with only electric field for electrostatic actuation also can cool the CPU (Figure 4b). The high cooling performance, compact structure, and convenient expansibility show that double-unit refrigeration device has a great potential in cooling of miniature integrated devices.

3. Conclusion

In summary, we have successfully fabricated a double-unit refrigeration device based on modified EC polymer, which is actuated by electrostatic force. The introduction of DOP effectively enhances the EC effect of relaxor ferroelectric polymer by improving the degrees of the freedom of the polymer molecular chains. The double-unit electrostatic-actuated refrigeration device made of modified P(VDF-TrFE-CFE) polymer stack achieves a maximum temperature span of 4.8 K . After 4500 times of repeated charging and discharging, there is no obvious cooling performance degradation of double-unit device. The experimental results show that the device can be activated at any time by automatic control circuit to regulate the temperature of CPU, in which the maximum cooling is 22.4 K . The double-unit refrigeration device, owing to the characteristics of miniaturization, high cooling performance, and low energy consumption, opens a way for the use of the EC refrigeration technology for thermal regulation of microelectronic devices.

4. Experimental Section

Preparation of CNTs Dispersion: Carboxylic SWNTs powder (5 mg , Nanjing/Jiangsu XFNANO Materials Tech Co., Ltd) was dispersed in a mixture of iso-propyl alcohol (18 mL) and deionized water (2 mL) using tip ultrasonic for 1 h . The dispersion was centrifuged at 3500 rpm for 5 min , and the supernatant was used as the precursor solution for spray-coating the CNT-based electrode.

Fabrication Process of EC Polymer Stack: P(VDF-TrFE-CFE) powder ($64.8/27.4/7.8 \text{ mol}\%$, Piezotech Arkema) and DOP were dissolved

at 20 wt% in 2-Butanone (Tianjin bohua Chemical Reagent Co. LTD, 99.0%) by stirring at 60 °C for 12 h, respectively. Then, two solutions were mixed in a certain proportion by stirring at 60 °C for 12 h. After that, the solution was filtered using a PTFE filter with a pore size of 0.22 μm. Before use, the filtered solution was degassed by bath ultrasonic to make a precursor solution of modified EC polymer. The precursor solution was blade-coated on a clean glass. Then, the substrate coated with the solution film was placed in a vacuum oven at 90 °C for 3 h to evaporate the solution. The CNT dispersion was spray-coated on EC polymer using a pre-defined 2 cm × 6 cm mask to form a conductive network. Another EC polymer was prepared by blade-coating precursor solution on CNT network. A part of CNT network was uncovered using to connect with supply power. The precursor solution covered substrate was placed in a vacuum oven at 90 °C for 3 h to evaporate the solution again. Next, the film was peeled off from the substrate carefully. Then, CNT dispersion was spray-coated on the rest of two surfaces of the film to form another two electrodes. The overlap of EC polymers and three CNT-based electrodes was defined as active area (2 cm × 4 cm in size) for the EC effect. Finally, as-prepared EC polymer stack was annealed in a vacuum oven at 120 °C for 10 h.

Fabrication of Double-Unit Refrigeration Device: The structure of double-unit refrigeration device, including two EC polymer stacks, is shown in Figure 2a. Before use, Cu wires were attached on all of CNT electrodes in two EC polymer stacks with transparent tape. In each unit, two 50-μm-thick PET films coated with graphene-paint electrode were separated by two 3-mm-thick PDMS spacers. In the case of the upper unit, a two-layer EC polymer stack was mounted on one end of the unit between the left spacer and the upper PET film, and the other end between the right spacer and the lower PET film. The state of the two-layer EC polymer stack in the lower unit was opposite to that in the upper unit. The adjacent PET films between each unit shared a graphene-paint electrode. Finally, single-sided PI tapes covered the outmost graphene-paint-coated PET film in the double-unit refrigeration device to electrically insulate the device from the heat source and the heat sink.

Characteristics of EC Polymer Stack: The cross-section morphology was observed using scanning electron microscope (JEOL, JSM-7800). The polarization-electric field loop of modified EC polymer was measured by a modified Sawyer–Tower circuit. X-ray diffraction data were achieved by X-ray powder diffraction instrument (Rigaku Smart Lab SE). The polarizing microscopy images were achieved using polarizing microscopic (SOPTOP, CX40P).

Measurement of Temperature Span: To obtain the temperature span, refrigeration device was placed on an Al block used as heat sink. The top graphene-paint electrode was directly exposed to the air without insulated PI film for infrared imaging. First, heat was pumped from top PET to the Al block under normal operating conditions. The time-resolved temperature of top electrode is the cooling curve. Then, an inverted device was placed on the Al block with unchanged control circuit. The original top electrode was insulated by PI film and the original bottom electrode was exposed to air for infrared imaging. That way, the heat was pumped from the Al block to the top electrode. The measured time-resolved temperature curve responses the heating curve in temperature span.

Calculation of COP and Specific Cooling Power: The COP is determined as $COP = \frac{\phi_{\text{heat flux}}}{W_{\text{energy consumption}}}$, where $\phi_{\text{heat flux}}$ and $W_{\text{energy consumption}}$ are the total heat flux and the total electric energy consumption of double-unit refrigeration device in one operation period, respectively. The heat flux ($\phi_{\text{heat flux}}$) was measured by heat flux sensor (Figure S6d, Supporting Information). The electric energy consumption of the double-unit refrigeration device can be calculated with $W_{\text{energy consumption}} = \int_{t_1}^{t_2} V \times I \, dt$, where V and I are the measured operating voltage and current, respectively (Figure S10, Supporting Information). t_1 and t_2 are the start and the end time of an entire operation period. The specific cooling power was equal to the ratio of the heat flux in an operation period and total mass of two-layer EC polymer stack.

Supporting Information

Supporting Information is available from the Wiley Online Library or from the author.

Acknowledgements

Y.B. and Q.Z. contributed equally to this work. This work was supported by National Key R&D Program of China (2020YFA0711500), the National Natural Science Fund of China (51973095 & 52011540401), “Fundamental Research Funds for the Central Universities”, Nankai University (023-92022018).

Conflict of Interest

The authors declare no conflict of interest.

Data Availability Statement

Research data are not shared.

Keywords

electrocaloric effect, electrostatic actuating, high efficiencies, microelectronics cooling, solid-state cooling

Received: December 4, 2020

Revised: January 15, 2021

Published online:

- [1] Z. Yan, J. Christofferson, A. Shakouri, Z. Gehong, J. E. Bowers, E. T. Croke, *IEEE Trans. Compon. Packag. Technol.* **2006**, 29, 395.
- [2] J. Y. Shi, D. L. Han, Z. C. Li, L. Yang, S. G. Lu, Z. F. Zhong, J. P. Chen, Q. M. Zhang, X. S. Qian, *Joule* **2019**, 3, 1200.
- [3] *Electrocaloric Materials: New Generation of Coolers*, (Eds: T. Correia, Q. M. Zhang), Springer, New York **2014**.
- [4] R. A. Kishore, A. Nozariasmar, B. Poudel, M. Sanghadasa, S. Priya, *Nat. Commun.* **2019**, 10, 1765.
- [5] S. Hong, Y. Gu, J. K. Seo, J. Wang, P. Liu, Y. S. Meng, S. Xu, R. K. Chen, *Sci. Adv.* **2019**, 5, eaaw0536.
- [6] S. Pourhedayat, *ACS Appl. Energy Mater.* **2018**, 229, 364.
- [7] Y. Liu, Y. Su, *Appl. Therm. Eng.* **2018**, 144, 747.
- [8] H. Ossmer, F. Wendler, M. Gueltig, F. Lambrecht, S. Miyazaki, M. Kohl, *Smart Mater. Struct.* **2016**, 25, 085037.
- [9] T. Tsukamoto, M. Esashi, S. Tanaka, *J. Micromech. Microeng.* **2012**, 22, 094008.
- [10] P. D. Thacher, *J. Appl. Phys.* **1968**, 39, 1996.
- [11] A. S. Mischenko, Q. M. Zhang, J. F. Scott, R. W. Whatmore, N. D. Mathur, *Science* **2006**, 311, 1270.
- [12] J. Li, Y. Chang, S. Yang, Y. Tian, Q. Hu, Y. Zhuang, Z. Xu, F. Li, *ACS Appl. Mater. Interfaces* **2019**, 11, 23346.
- [13] B. Nair, T. Usui, S. Crossley, S. Kurdi, G. G. Guzman-Verri, X. Moya, S. Hirose, N. D. Mathur, *Nature* **2019**, 575, 468.
- [14] U. Plaznik, A. Kitanovski, B. Rožič, B. Malič, H. Uršič, S. Drnovšek, J. Cilenšek, M. Vrabelj, A. Poredoš, Z. Kutnjak, *Appl. Phys. Lett.* **2015**, 106, 043903.
- [15] Y. Wang, D. E. Schwartz, S. J. Smullin, Q. Wang, M. J. Sheridan, *J. Microelectromech. Syst.* **2017**, 26, 580.

- [16] Y. V. Sinyavsky, V. M. Brodyansky, *Ferroelectrics* **1992**, *131*, 321.
- [17] Y. B. Jia, Y. S. Ju, *Appl. Phys. Lett.* **2012**, *100*, 242901.
- [18] B. Neese, B. J. Chu, S. G. Lu, Y. Wang, E. Furman, Q. M. Zhang, *Science* **2008**, *321*, 821.
- [19] X. Li, X. S. Qian, S. G. Lu, J. Cheng, Z. Fang, Q. M. Zhang, *Appl. Phys. Lett.* **2011**, *99*, 052907.
- [20] R. J. Ma, Z. Y. Zhang, K. Tong, D. Huber, R. Kornbluh, Y. S. Ju, Q. B. Pei, *Science* **2017**, *357*, 1130.
- [21] Y. Meng, Z. Y. Zhang, H. X. Wu, R. Y. Wu, J. H. Wu, H. L. Wang, Q. B. Pei, *Nat. Energy* **2020**, *5*, 996.
- [22] J. Qian, M. Guo, J. Jiang, Z. Dan, Y. Shen, *J. Mater. Chem. C* **2019**, *7*, 3212.
- [23] Q. Li, G. Z. Zhang, X. S. Zhang, S. L. Jiang, Y. Zeng, Q. Wang, *Adv. Mater.* **2015**, *27*, 2236.
- [24] G. Z. Zhang, X. S. Zhang, T. N. Yang, Q. Li, L. Q. Chen, S. L. Jiang, Q. Wang, *ACS Appl. Nano Mater.* **2015**, *9*, 7164.
- [25] L. Yang, X. S. Qian, C. Koo, Y. Hou, T. Zhang, Y. Zhou, M. Lin, J. H. Qiu, Q. M. Zhang, *Nano Energy* **2016**, *22*, 461.
- [26] J. F. Qian, R. Peng, Z. H. Shen, J. Y. Jiang, F. Xue, T. N. Yang, L. Q. Chen, Y. Shen, *Adv. Mater.* **2019**, *31*, 1801949.
- [27] Y. Q. Chen, J. F. Qian, J. Y. Yu, M. F. Guo, Q. H. Zhang, J. Y. Jiang, Z. H. Shen, L. Q. Chen, Y. Shen, *Adv. Mater.* **2020**, *32*, 1907927.
- [28] X. S. Qian, H. J. Ye, T. N. Yang, W. Z. Shao, L. Zhen, E. Furman, L. Q. Chen, Q. M. Zhang, *Adv. Funct. Mater.* **2015**, *25*, 5134.
- [29] X. Z. Chen, X. S. Qian, X. Li, S. G. Lu, H. M. Gu, M. Lin, Q. D. Shen, Q. M. Zhang, *Appl. Phys. Lett.* **2012**, *100*, 222902.
- [30] L. Engel, S. Kruk, J. Shklovsky, Y. Shacham-Diamand, S. Krylov, *J. Micromech. Microeng.* **2014**, *24*, 125027.
- [31] J. F. Scott, *Annu. Rev. Mater. Sci.* **2011**, *41*, 229.
- [32] L. Zhu, Q. Wang, *Macromolecules* **2012**, *45*, 2937.
- [33] R. Casalini, K. L. Ngai, C. G. Robertson, C. M. Roland, *J. Polym. Sci., Part B: Polym. Phys.* **2000**, *38*, 1841.
- [34] E. H. Immergut, H. F. Mark, in *Principles of Plasticization*, American Chemical Society, Washington, DC **1965**, pp. 1–26.
- [35] J. F. Qian, J. Y. Jiang, Y. Shen, *J. Materiomics* **2019**, *5*, 357.